SUBJECT: **SPIRE FTS Instrument RSRF Derivation**

PREPARED BY: **Trevor Fulton**

DOCUMENT No: **SPIRE-BSS-REP-003261**

ISSUE: **Issue 1.0** **Date:** **17 March 2011**

APPROVED BY: **Date:**

Distribution

Name

Edward Polehampton
Trevor Fulton
Peter Imhof
Michael Pohlen

Change Record

ISSUE	DATE	Changes
Draft 0.1	03 February 2011	First version
Issue 1.0	17 March 2011	First released version

TABLE OF CONTENTS

Glossary

CR	Calibration Resolution
FT	Fourier Transform
HR	High Resolution
LHS	Left Hand Side
LR	Low Resolution
MR	Medium Resolution
NHKT	Nominal Housekeeping Timeline Product
OD	Operational Day
RHS	Right Hand Side
RSRF	Relative Spectral Response Function
SDI	Spectrometer Detector Interferogram Product
SDS	Spectrometer Detector Spectrum Product
SDT	Spectrometer Detector Timeline Product
SMECT	Spectrometer MEChanism Timeline Product
SLW	Spectrometer Long Wavelength array
SMEC	Spectrometer MEChanism
SNR	Signal to noise ratio
SPIRE	Spectral and Photometric Imaging REceiver
SSW	Spectrometer Short Wavelength array
TBD	To Be Determined
TBW	To Be Written

1. INTRODUCTION

The purpose of this document is to describe the method used to derive the Instrument RSRF calibration curves for each of the SPIRE FTS detectors.

1.1 Documents

1.1.1 Applicable Documents

Number	Document Title	Author(s)	Issue
AD01	SPIRE Spectrometer Pipeline Description	Trevor Fulton	1.2
AD02	Dark Sky spectra evolution with time	Jean-Paul Baluteau	1, 2
AD03	Flux Conversion and RSRF correction for the SPIRE FTS	Trevor Fulton, Edward Polehampton, Jean-Paul Baluteau, Bruce Swinyard	1.0
AD04	SPIRE FTS Update: Telescope/Instrument Correction, Presentation to the SPIRE SDAG, 18 Feb. 2010	Trevor Fulton	

2. BACKGROUND

The spectrum recorded by the SPIRE FTS when observing any astronomical source, $V_{Meas}(\sigma)$, can be expressed as a linear combination of contributions from three distinct entities: the astronomical source itself, $V_{source}(\sigma)$; the Herschel Telescope, $V_{Tele}(\sigma)$; and the SPIRE Instrument (FPU and SCAL), $V_{Inst}(\sigma)$ (see AD01 eq. 3.41).

$$V_{Meas}(\sigma) = V_{source}(\sigma) + V_{Tele}(\sigma) + V_{Inst}(\sigma) \quad \text{(Error! Bookmark not defined.2.1)}$$

Consider an observation that is common to the SPIRE FTS calibration plan; that of the Dark Astronomical sky. The spectrum of these data contains no contribution from an astronomical source and therefore the measured spectrum, $V_{Dark}(\sigma)$, may be expressed as in eq. 2.2:

$$V_{Dark}(\sigma) = V_{Tele}(\sigma) + V_{Inst}(\sigma) \quad \text{(Error! Bookmark not defined.2.2)}$$

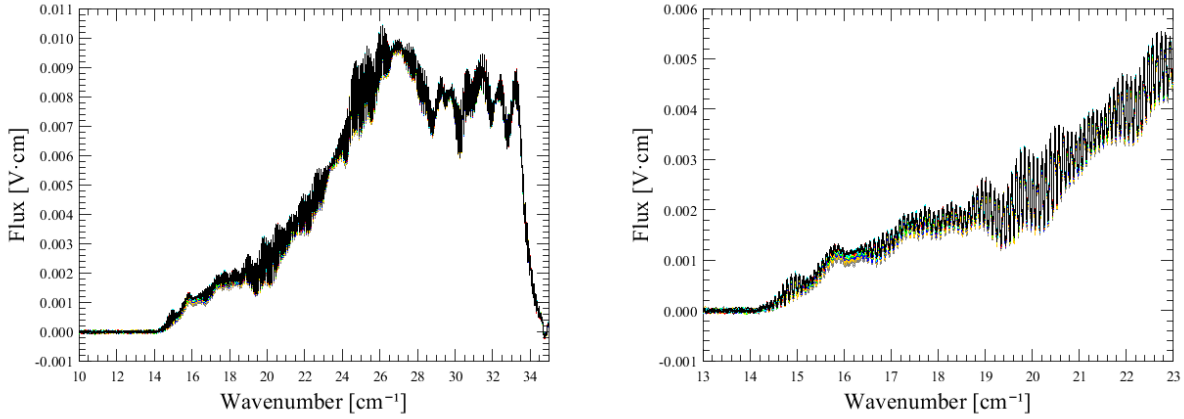

Figure 1: **Measured spectrum, $V_{Dark}(\sigma)$, for detector SLWC3, including the Telescope $V_{Tele}(\sigma)$, and Instrument $V_{Inst}(\sigma)$ contributions**. Left: Full pass band; right: close-up of the long wavelength region.

The spectra measured for a Dark Astronomical Sky observation (OBSID=0x50002C81, N_{Reps}=40 or N_{Scans}=80), $V_{Dark\text{-}n}(\sigma)$, for detector SLWC3 are shown in Figure 1. As can be seen in both plots, but in particular in the close-up view, there is some systematic spectrum-to-spectrum deviation, most prominently in the long wavelength region.

Next, consider the plots shown in Figure 2. There, the values of SCAL cavity thermometer and the scan numbers are shown for observation 0x50002C81 as a function of time.

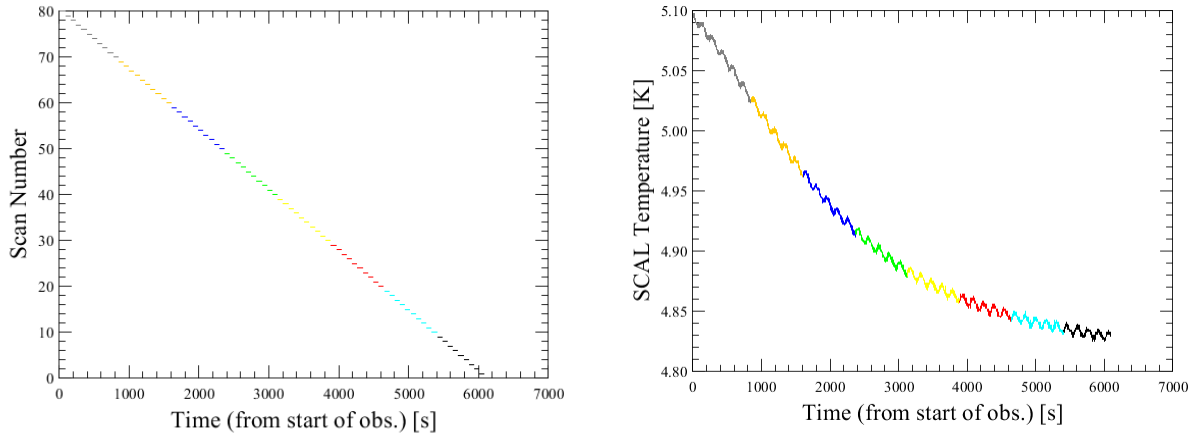

Figure 2: **Nominal Housekeeping parameters for observation 0x50002C81**. Left, SMEC scan number vs. time; right, SCAL Temperature vs. time.

The plots in Figure 2 show that the temperature SPIRE Instrument (FPU, SCAL cavity), represented by the SCAL cavity thermometer, itself varied over the course of the Dark sky observation 0x50002C81. This leads to a first-order model for the spectral contribution of the SPIRE Instrument, $V_{Inst}(\sigma)$. In this first-order model, $V_{Inst}(\sigma)$ is expressed as a product of an emission from a blackbody source and a relative spectral response function (RSRF) as in eq. 2.3,

$$V_{Inst}(\sigma) = R_{Inst}(\sigma) B_{Inst}(\sigma). \qquad (2.3)$$

The emission from the SPIRE Instrument (FPU, SCAL cavity) is combined into a single emitting term, $B_{Inst}(\sigma)$, as in eq. 2.4,

$$B_{Inst}(\sigma) = B(T_{Inst}, \sigma)\,, \tag{2.4}$$

where $B(T,\sigma)$ is the Planck function,

$$B(T,\sigma) = \frac{2h(100c\sigma)^3}{c^2}\frac{1}{e^{h100c\sigma/kT}-1} \tag{2.5}$$

and T_{Inst} is the average of the values of the SCAL thermometer recorded over the course of a given scan of the Spectrometer Mechanism (see Figure 2).

3. INSTRUMENT RSRF

Equation 2.4 represents one term of the overall instrument model, $V_{Inst}(\sigma)$. The other portion of the instrument model is the Instrument RSRF, $R_{Inst}(\sigma)$. Consider again the plots in Figure 1 that show the measured spectra for each scan n of the Dark Sky observation; i.e. $V_{Dark\text{-}n}(\sigma)$. Each of these spectra may be represented as a combination of eqs. 2.2 and 2.3,

$$V_{Dark-n}(\sigma) = V_{Tele-n}(\sigma) + R_{Inst}(\sigma)\times B(T_{Inst-n},\sigma)\,. \tag{3.1}$$

Next, consider the spectrum of a single scan, k, of the dark sky observation, $V_{Dark\text{-}k}(\sigma)$. The difference between and given measured spectrum, $V_{Dark\text{-}n}(\sigma)$, and the measured spectrum for scan k, $V_{Dark\text{-}k}(\sigma)$, may be expressed as,

$$\begin{aligned} V_{Dark-n}(\sigma) - V_{Dark-k}(\sigma) &= \left[V_{Tele-n}(\sigma) + R_{Inst}(\sigma)\times B(T_{Inst-n},\sigma)\right] \\ &\quad - \left[V_{Tele-k}(\sigma) + R_{Inst}(\sigma)\times B(T_{Inst-k},\sigma)\right] \\ &= \left[V_{Tele-n}(\sigma) - V_{Tele-k}(\sigma)\right] \\ &\quad + \left[R_{Inst}(\sigma)\times B(T_{Inst-n},\sigma) - R_{Inst}(\sigma)\times B(T_{Inst-k},\sigma)\right] \end{aligned}\,. \tag{3.2}$$

If one assumes that the spectral contribution from the Herschel Telescope is constant from scan to scan over the course of an observation, then eq. 3.2 may be reduced to

$$V_{Dark-n}(\sigma) - V_{Dark-k}(\sigma) = R_{Inst}(\sigma)\times\left[B(T_{Inst-n},\sigma) - B(T_{Inst-k},\sigma)\right]. \tag{3.3}$$

By way of illustration, consider again the Dark sky observation 0x50002C81 and let k=40 for even values of n and k=41 for odd values of n,

$$\begin{aligned} V_{Dark-n_{even}}(\sigma) - V_{Dark-40}(\sigma) &= R_{Inst}(\sigma)\times\left[B(T_{Inst-n_{even}},\sigma) - B(T_{Inst-40},\sigma)\right] \\ V_{Dark-n_{odd}}(\sigma) - V_{Dark-41}(\sigma) &= R_{Inst}(\sigma)\times\left[B(T_{Inst-n_{odd}},\sigma) - B(T_{Inst-41},\sigma)\right] \end{aligned}\,. \tag{3.4}$$

The spectral differences given by eq. 3.4 are shown in Figure 3.

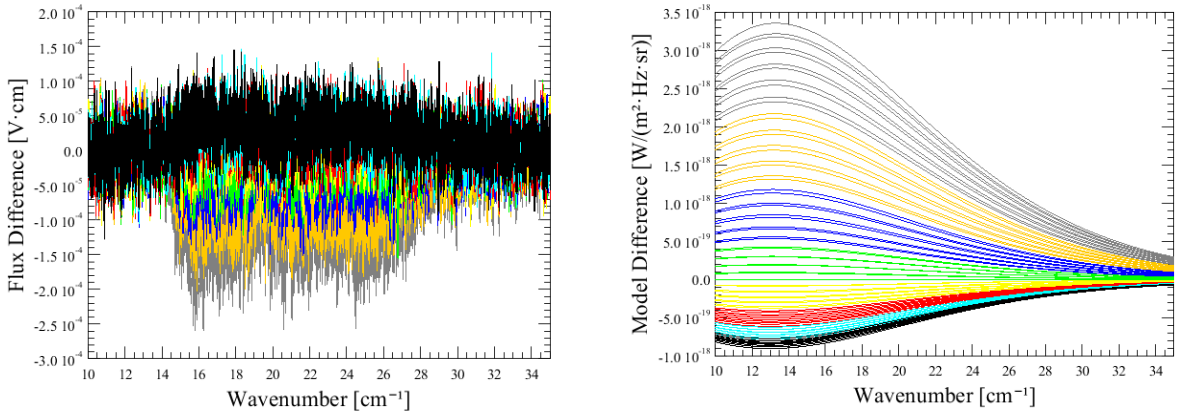

Figure 3: **Spectral differences for detector SLWC3, OBSID-0x50002C81**. Left: Measured spectra, $V_{Dark\text{-}n}(\sigma)$- $V_{Dark\text{-}k}(\sigma)$; Instrument emission, $B(T_{Inst\text{-}n}, \sigma)$- $B(T_{Inst\text{-}k}, \sigma)$.

Next, instead of using a single scan k (per scan direction) as the reference scan, the observation is divided into two halves – one half that contains scans where $n \geq N_{Scans}/2$, the other that contains scans where $n < N_{Scans}/2$. The spectral differences expressed in eq. 3.3 now become

$$V_{Dark-n}(\sigma) - V_{Dark-(n-N_{Scans}/2)}(\sigma) = R_{Inst}(\sigma) \times \left[B(T_{Inst-n}, \sigma) - B(T_{Inst-(n-N_{Scans}/2)}, \sigma) \right], \qquad (3.5)$$

The spectral half-differences given by eq. 3.5 are shown in Figure 4.

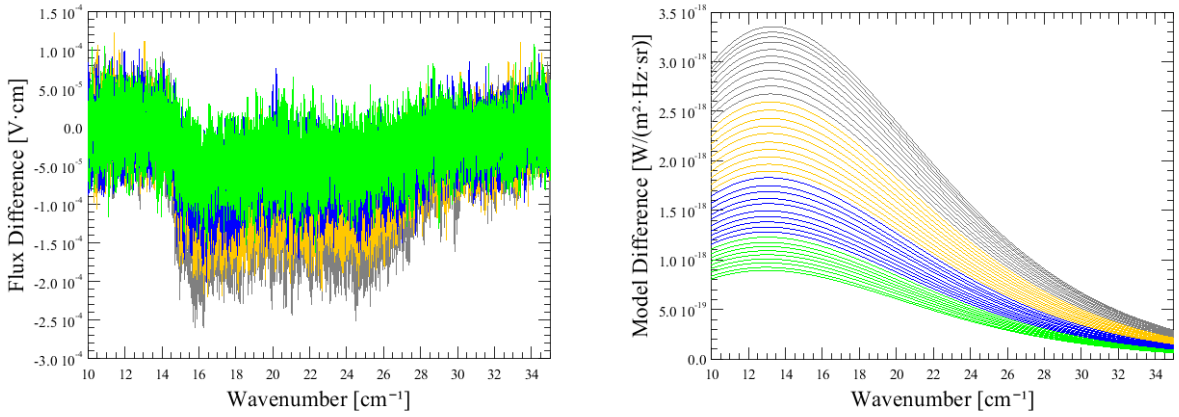

Figure 4: **Spectral half-differences for detector SLWC3, OBSID-0x50002C81**. Left: Measured spectra, $V_{Dark\text{-}n}(\sigma)$- $V_{Dark\text{-}(n\text{-}NScans/2)}(\sigma)$; Instrument emission, $B(T_{Inst\text{-}n}, \sigma)$- $B(T_{Inst\text{-}(n\text{-}NScans/2)}, \sigma)$.

The Instrument RSRF, $R_{Inst}(\sigma)$, may be isolated by rearranging eq. 3.5. These Instrument RSRFs (eq. 3.6) for detector SLWC3, OBSID=0x50002C81, are shown in Figure 5.

$$R_{Inst}(\sigma) = \frac{V_{Dark-n}(\sigma) - V_{Dark-(n-N_{Scans}/2)}(\sigma)}{B(T_{Inst-n}, \sigma) - B(T_{Inst-(n-N_{Scans}/2)}, \sigma)}. \qquad (3.6)$$

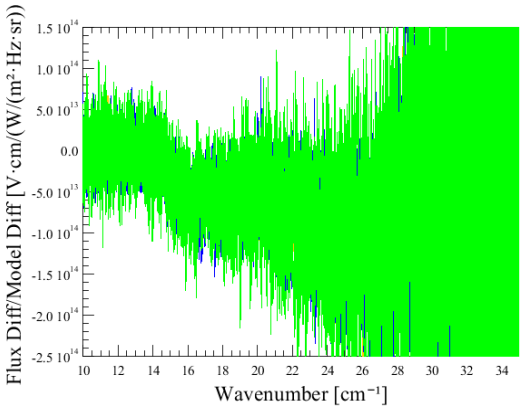

Figure 5: **Empirical Derivation of the Instrument RSRF**. OBSID=0x50002C81, detector=SLWC3, derived using half differences.

4. INSTRUMENT RSRF CALIBRATION CURVES

In principle, the measured spectra from every SPIRE FTS observation of the Dark Astronomical sky may be used to derive the Instrument RSRF calibration curves given by eq. 3.6. Indeed, if the stability of the Telescope pointing is such that the spectral contribution from the Astronomical target does not vary measurably over the course of an observation, then *all* SPIRE FTS observations may be used to derive $R_{Inst}(\sigma)$. Moreover, since each $R_{Inst}(\sigma)$ curve is essentially normalized, a single $\overline{R_{Inst}(\sigma)}$ curve for each SPIRE FTS detector may be computed as the average of all of the individual $R_{Inst}(\sigma)$ curves (see eq. 4.1).

As a start, and adopting a conservative approach, only FTS observations of the Dark Astronomical sky shall be considered as candidates. In addition, the choice of Dark sky observations shall be limited to those whose instrument temperature profile (see Figure 2) is similar to that of OBSID=0x50002C81. The reason for this secondary restriction is to maximize the Temperature spread between each half-difference, thereby maximizing the S/N of each $R_{Inst}(\sigma)$ curve. Finally, the SMEC scan direction shall be taken into account in the derivation of the Instrument RSRF curves for each SPIRE FTS detector; e.g. each detector will have one calibration curve per scan direction.

Based on the aforementioned conditions, six SPIRE FTS observations have been identified as being appropriate for the empirical derivation of the Instrument RSRF curves and are listed in Table 1.

OBSID	OD	Target	Resolution	N_{reps}	M1 [K]	M2 [K]
0x50002AA3	217	Dark Sky	CR	50	88.0534	84.2699
0x50002C81	227	Dark Sky	CR	40	88.1561	84.3814
0x50002E40	240	Dark Sky	CR	40	88.2620	84.4789
0x50002FE5	250	Dark Sky	CR	50	88.5967	84.7139
0x50003144	261	Dark Sky	CR	50	88.7189	84.8548
0x50004ED0	383	Dark Sky	CR	50	88.1760	84.2882

Table 1: Dark Sky observations used to derive the Instrument RSRF ($R_{Inst}(\sigma)$) calibration curves. Note that the temperatures listed for M1 and M2 are time averages of nine and three thermometers, respectively, over the course of the observation.

The SPIRE Instrument temperature profiles for each observations listed in Table 1, given by the recorded values of the SCALTEMP thermometer are shown in Figure 6.

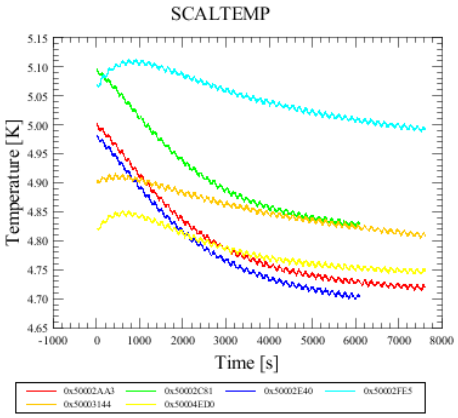

Figure 6: **SCAL Temperatures.** The curves shown here are the recorded values of the SCAL Cavity thermometer for the Dark sky observations used to derived the Instrument RSRF calibration curves.

The Instrument RSRF curves for each detector and for each SMEC scan direction are computed as the averages of all of the individual half-difference RSRF curves from each of the candidate Dark sky observations (eq. 4.1). Since each of the candidate observations were performed in Calibration resolution mode (CR) and since each of the nominal SPIRE FTS spectral resolutions (LR, MR, HR) are subsets of CR, the measured spectra from the observations listed in may additionally be used to derive Instrument RSRF curves for each of the nominal SPIRE FTS spectral resolutions. The calibration curves for the SLW detectors for each of the nominal spectral resolutions are shown in Figure 7, Figure 8, and Figure 9.

$$\overline{R_{Inst}(\sigma)} = \sum_{n=N_{Scans}/2}^{N_{Scans}} R_{Inst-n}(\sigma) = \sum_{n=N_{Scans}/2}^{N_{Scans}} \left[\frac{V_{Dark-n}(\sigma) - V_{Dark-(n-N_{Scans}/2)}(\sigma)}{B(T_{Inst-n},\sigma) - B(T_{Inst-(n-N_{Scans}/2)},\sigma)} \right]. \qquad (4.1)$$

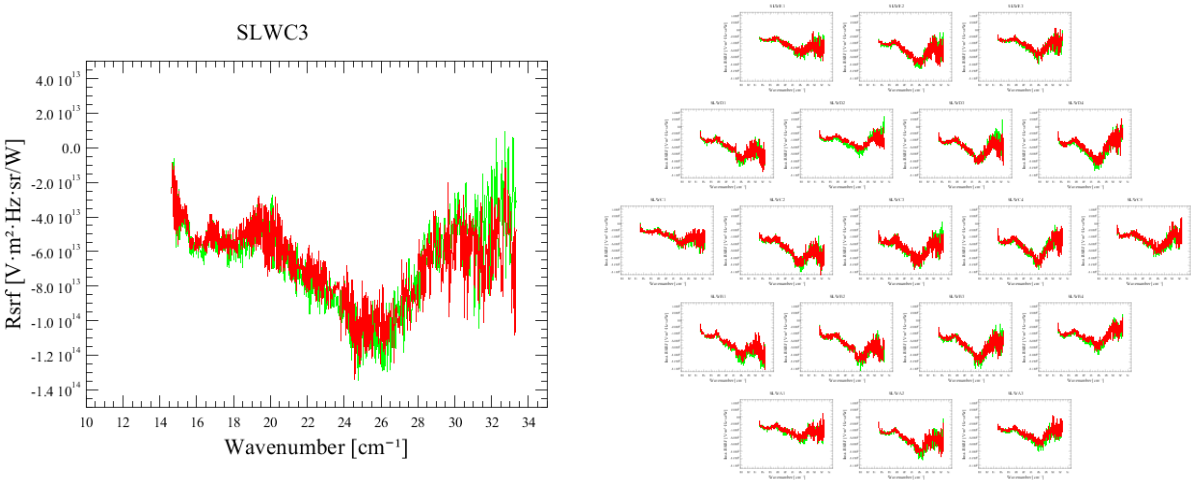

Figure 7: **Instrument RSRF calibration curves, High spectral resolution.** Left: SLWC3; right: All SLW detectors. The green curves apply to forward SMEC scans, the red curves apply to reverse SMEC scans.

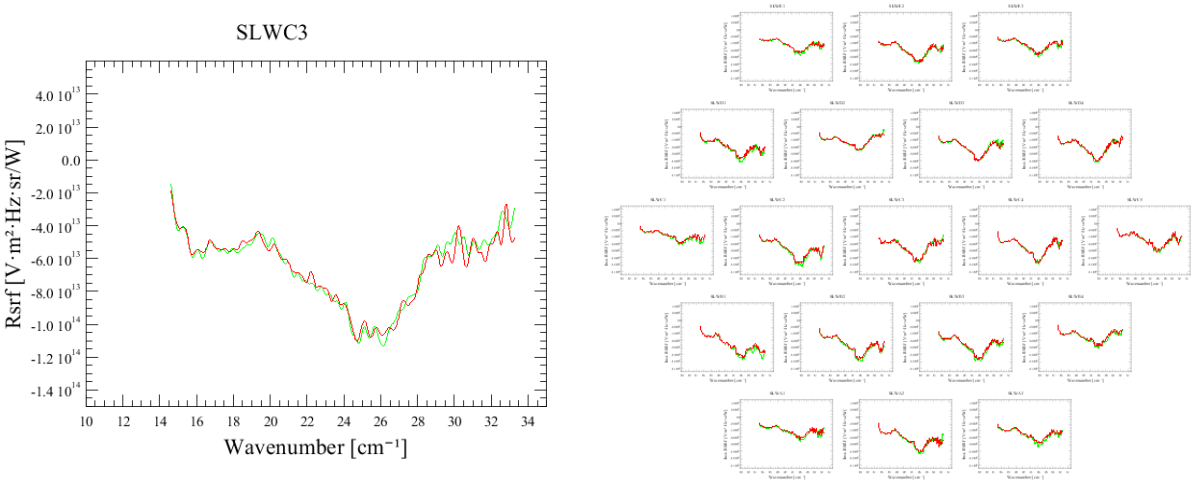

Figure 8: **Instrument RSRF calibration curves, Medium spectral resolution.** Left: SLWC3; right: All SLW detectors. The green curves apply to forward SMEC scans, the red curves apply to reverse SMEC scans.

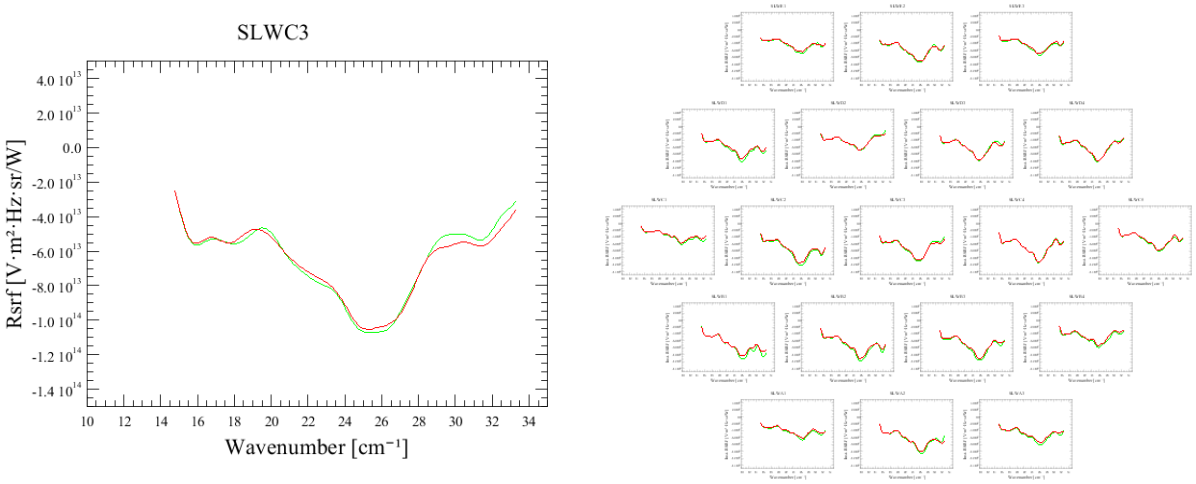

Figure 9: **Instrument RSRF calibration curves, Low spectral resolution.** Left: SLWC3; right: All SLW detectors. The green curves apply to forward SMEC scans, the red curves apply to reverse SMEC scans.